6TH INTERNATIONAL CONFERENCE ON FLOOD MANAGEMENT
September 2014 - São Paulo - Brazil
ICFM6

METHOD FOR DEVELOPING HAZARD MAP DUE TO DEBRIS FLOW PREDICTION

R. Escalona[1&2], A. Yorozuya[3], S. Egashira[3] and Y. Iwami[3]
1. *San Felipe Mayoralty, Venezuela.*
2. *Association of Ex-Students of Japan International Corporation Agency, Venezuela (JICA-Venezuela).*
3. *International Centre for Water Hazard and Risk Management (ICHARM) under the auspices of UNESCO.*

ABSTRACT: This study aims to propose a method for developing hazard maps due to debris flow based on numerical simulations with 1-D and 2-D debris flow models. The 1-D numerical simulations were conducted to investigate variables responsible to debris flow volume. 2-D numerical simulations were performed to analyze the debris flow behavior over ideal debris fans, as well as to obtain basic information necessary for preparing a hazard map. The 1-D numerical results show that the debris flow volume increases with supply water discharge, length of stream reach and bed slope in condition that potential erosion depth is large enough for sediment transport capacity of debris flow, and that the debris flow size reaches its equilibrium after flowing over some distance. The 2-D numerical results show that debris flow spreading increases longitudinally with the fan slope and in addition, a hazardous area, which is usually considered as deposition area, is reproduced in response to the ground surface topography of the fan, although there is an artificial channel for draining flood water.

Key Words: Debris flow, 1-D numerical simulation, 2-D numerical simulation, hazard map.

1. INTRODUCTION

Every year, mass communication and bulletins of international institutions show the sediment related disasters that occur worldwide, where they are reflected numbers of high deaths and economic losses. Some countries have made progress in reducing the impact of sediment related disasters because they have conducted prevention and mitigation measures for vulnerability reduction in areas of the high risk. To evaluate hazardous areas related to mass movements such as landslides and debris flow corresponding numerical models which are based on 1-D and 2-D governing equations are useful (Egashira *et al.* 1997, 2003, 2007; García *et al.* 2003, Takahashi *et al.* 2001, Takahashi 2007). The governing equations to describe debris flow behavior are composed of mass and momentum conservation equations for debris flow body as well as of mass conservation equation for bed sediment. Egashira *et al.* (1997, 2003) and Takahashi *et al.* (2001) introduced erosion and deposition terms into the mass conservation equation of debris flow body and bed sediment in order to evaluate influence of change of sediment mass on debris flow behavior. However, there are quite differences between their formulas for erosion and deposition rate formula (Egashira 2007, 2011). Bed shear stress formula which plays an important role in momentum conservation equation has been studied with constitutive relations of water and sediment mixture. Although several formulas have been proposed, their structural form is different to each other (Egashira 2007, 2011).

López *et al*. 2002 showed a methodology to create hazard map based on Flo-2D model developed by O'brien *et al.* (1993). 2-D Saint Venant equations for non-Newtonian fluids are employed in this model, and the procedure includes criteria to evaluate hazard as a function of the event intensity and frequency. JICA, 2004 integrated this model with the Japanese Law and delimited also hazard level with two criteria. Takahashi (2007) reproduced sediment flooding numerically with his colleagues' numerical model (2011). Mergily (2008) proposed an integrated modeling of debris flow with Open Source GIS and showed the intermediate characteristics between landslide and sediment runoff.

Present study aims to propose a method to develop hazard maps due to debris flow. 1-D and 2-D governing equations are described briefly with bed shear stress formula and erosion/ deposition rate formula. Discussions are made on the relation between debris flow volume and hydraulic variables such as bed slope, channel length, potential erosion depth and supplying water discharge based on 1D numerical simulations. In addition, debris flow flooding process is discussed using results obtained from 2-D numerical simulations. Finally a numerical simulation of debris flow is conducted, for the first step to develop the hazard map, focusing on the debris fan of a Chacaito creek located in Caracas city, Venezuela.

2. GOVERNING EQUATIONS EMPLOYED IN NUMERICAL MODELS

2.1 One dimensional governing equations

The 1-D governing equations are constituted by mass conservation of a sediment-water mixture, the momentum conservation of the mixture, and mass conservation of bed sediment. The mass conservation of debris flow is divided into two; one for the mixture and other for sediment only:

$$\frac{\partial h}{\partial t}+\frac{1}{B}\frac{\partial h\bar{u}B}{\partial x}=\frac{E}{c_*} \qquad [1] \qquad \frac{\partial \bar{c}h}{\partial t}+\frac{1}{B}\frac{\partial h\gamma\bar{c}\bar{u}B}{\partial x}=E \qquad [2]$$

The momentum conservation equation is described as follows, neglecting the term with derivative of mass density:

$$\frac{\partial h\bar{u}}{\partial t}+\frac{1}{B}\frac{\partial \beta h\overline{uu}B}{\partial x}=-gh\frac{\partial H}{\partial x}-\frac{\tau_b}{\rho_m} \qquad [3] \qquad \text{where} \qquad H=z_b+h\cos\theta \qquad [4]$$

The mass conservation of bed sediment is transformed into volumetric continuity:

$$\frac{\partial z_b}{\partial t}=-\frac{E}{c_*\cos\theta} \qquad [5]$$

In these equations, t is the time, x- is the coordinate along the flow direction, h is the flow depth, $\bar{u}$ is the spatial average velocity, B is the flow width, $\bar{c}$ is the spatial average sediment concentration, z_b is the bed elevation measured from a datum line, g is the acceleration due to gravity, E is the erosion rate or erosion velocity, τ_b is the bed shear stress, $\overline{\rho_m}$ is mass density defined as $\overline{\rho_m}=(\sigma-\rho)\bar{c}+\rho$ where σ is the mass density of sediment particle, ρ is the mass density of the water including fine sediment, and θ is the bed slope, c_* is the sediment concentration of stationary sediment layer, γ is the correction parameter for sediment transport rate, β is the momentum correction factor and H is the elevation of the free surface of the flow body.

2.2 Two dimensional governing equations

In the 2-D governing equations, the mass conservation equation of the flow body is also broken down into two equations (Egashira *et al*. 1997)

$$\frac{\partial h}{\partial t}+\frac{\partial uh}{\partial x}+\frac{\partial vh}{\partial y}=\frac{E}{c_*} \qquad [6] \qquad \frac{\partial \bar{c}h}{\partial t}+\frac{\partial \gamma\bar{c}uh}{\partial x}+\frac{\partial \gamma\bar{c}vh}{\partial y}=E \qquad [7]$$

x- and y- components of momentum conservation equations are as follow:

$$\frac{\partial uh}{\partial t}+\frac{\partial \beta uuh}{\partial x}+\frac{\partial \beta vuh}{\partial y}=-gh\frac{\partial H}{\partial x}-\frac{\tau_{bx}}{\rho_m} \quad [8] \qquad \frac{\partial uh}{\partial t}+\frac{\partial \beta uvh}{\partial x}+\frac{\partial \beta vvh}{\partial y}=-gh\frac{\partial H}{\partial x}-\frac{\tau_{by}}{\rho_m} \quad [9]$$

In the 2-D numerical simulation, erosion of bed sediment is neglected. However, the deposition process in the debris fans was included.

In these equations、τ_{bx} is the bed shear stress in x- component, τ_{by} is the bed shear stress in y-component, u is the depth averaged velocity in x- component and v is the depth averaged velocity in y-component.

2.3 Formulas for erosion rate and bed shear stress

The erosion rate is described by Egashira *et al.* (2001);

$$\frac{E}{|u|}=c_*\tan(\theta-\theta_e) \quad [10] \qquad \text{where} \qquad \tan\theta_e=\frac{\left(\sigma/\rho-1\right)\bar{c}}{\left(\sigma/\rho-1\right)\bar{c}+1}\tan\phi_s \quad [11]$$

in which E is the erosion and deposition rate ($E < 0$: deposition), θ is the local bed slope, and θ_e is the equilibrium bed slope corresponding to spatial average sediment concentration of the debris flow body, and ϕ_s is the inter-particle friction angle of sediment particles.

Egashira, *et al.(*2003) formulated the shear stress as follows.

$$\tau_0=\tau_{0y}+\rho f_b\bar{u}^2 \quad [12]$$

in which τ_0 is the bed shear stress, τ_{0y} is Coulomb type's shear stress and f_b is the friction factor associated fluid.

$$\tau_{0y}=\left(\frac{c}{c_*}\right)^{1/5}(\sigma-\rho)\,\bar{c}gh\cos\theta\tan\phi_s \quad [13]$$

Concerning about the friction f_b, Itoh *et al.* 2003 expressed the friction factor to simulate the whole flow regime. For example, Egashira *et al*. 2007 indicated the schematic diagram of the distribution of water/sediment in different regime as shown in Figure 1. They can be clarified as *h/hs*; e.g., when *h/hs* = 1, the flow regime is the debris flow as shown in figure 1(a), and when *h/hs* < 1, the flow regime is the flood flow in Figure 1(b), where h is total water depth, and h_s is thickness of sediment layer.

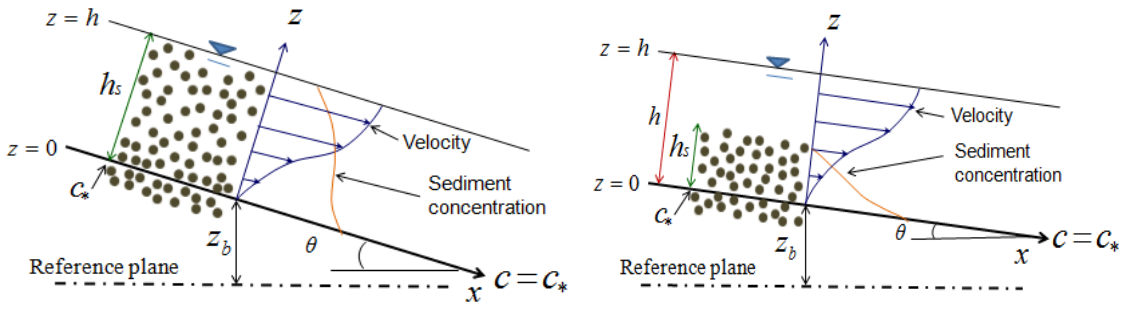

a) b)

Figure 1: Profiles of velocity and sediment concentration in (a) debris flow and (b) flood flow.

When h_s/h = 1 as shown in Figure 1(a) as the debris flow, it is the flow where sediment layer reaches to the top of water surface. In such a flow, the friction can be determined with h/d, sediment concentration and friction angle. Therefore, it can be expressed as:

$$f_b = \frac{25}{4}\left(f_d + f_f\right)\left(\frac{h}{d}\right)^{-2} \qquad [14]$$

in which f_d and f_f are defined as

$$f_d = k_d \left(\sigma/\rho\right)\left(1-e^2\right)\bar{c}^{\,1/3} \qquad [15] \qquad \text{and} \qquad f_f = \frac{k_f\left(1-\bar{c}\right)^{5/3}}{\bar{c}^{\,2/3}} \qquad [16]$$

In these relations, d is the reference sediment size, e is the restitution coefficient of sediment particles which is estimated at about 0.85, k_f and k_d are the coefficient determined by flume test and specified as k_f = 0.16 and k_d = 0.0828.

When h_s/h < 1 as shown in Figure 1(b), it is the flow as the flood flow including the water and sediment as bedload. In such a flow, it is necessary to consider an additional term of h_s/h from the case when hs/h = 1 (Itoh, *et al* 2003).

$$f_b = \left[1-\left(\frac{c_s}{c_*}\right)^{1/5}\right] GK^{-2}\left(\frac{h}{d}\right)^{-2} \qquad [17]$$

where K and G are defined as $K = K_s + K_i + K_w$ [18]

and $G = \left(\sigma/\rho - 1\right)\bar{c} + 1$ [19] respectively K_w, K_i and K_s are defined as follow:

$$K_w = \frac{1}{k}\sqrt{1-\frac{\bar{c}}{c_s}}\left(\frac{\eta_0}{h}+1-\frac{\bar{c}}{c_s}\right)\left(\frac{h}{d}\right)^{-1}\ln\left\{\frac{\frac{\eta_0}{h}+1+\frac{\bar{c}}{c_s}}{\frac{\eta_0}{h}}\right\} - \frac{1}{k}\left(1-\frac{\bar{c}}{c_s}\right)^{3/2}\left(\frac{h}{d}\right)^{-1} \qquad [20]$$

$$K_s = \frac{4}{15}r^{-2}\left(f_{ds}+f_{fs}\right)^{-0.5}\left[\left(1-\frac{\bar{c}}{c_s}\right)^{5/2} - \left\{\left(1-\frac{\bar{c}}{c_s}\right)+r\frac{\bar{c}}{c_s}\right\}^{3/2}\left\{\left(1-\frac{\bar{c}}{c_s}\right)-1.5r\frac{\bar{c}}{c_s}\right\}\right] \qquad [21]$$

$$K_i = -\frac{2}{3}r^{-1}\left(f_{ds}+f_{fs}\right)^{-0.5}\left(1-\frac{\bar{c}}{c_s}\right)\left[\left(1-\frac{\bar{c}}{c_s}\right)^{3/2} - \left\{\left(1-\frac{\bar{c}}{c_s}\right)+r\frac{\bar{c}}{c_s}\right\}^{3/2}\right] \qquad [22]$$

$$f_{ds} = k_d\left(\sigma/\rho\right)\left(1-e^2\right)c_s^{\,1/3} \qquad [23] \qquad f_{fs} = k_f\left(1-c_s\right)^{5/3}c_s^{\,-2/3} \qquad [24]$$

$$r = 1+\left(c_s/\bar{c}\right)\left[\left\{1-\left(c_s/c_*\right)^{1/5}\right\}G-1\right] \qquad [25]$$

In the Eq. [20], k is Karman constant, and η_0 is the mixing length at the interface between the water-sediment mixture layer and the upper water layer. This term is defined as following (Egashira *et al.* 1997).

$$\eta_0 = al_0 = \sqrt[a]{k_f}\left\{\left(1-c_s\right)\Big/c_s\right\}^{1/3} d \qquad a \cong 1.0 \qquad [26]$$

The specific sediment concentration in the layer of hyper-concentrated sediment-water mixture is estimated as $c_s = c_* / 2$.

3. SIMILATION OF DEBRIS FLOW BEHAVIOR

3.1 1-D Numerical simulation

3.1.1 Initial and Boundary condition

The initial and the boundary condition are determined as Table 1 as well as the physical parameters, such as σ = 2,650 kg/m^3, ρ = 1,000 kg/m^3, ϕ_s = 34°, c_* = 0.52. The calculation conditions are that the flow width B = 15.00 m, Δx = 5.00 m, and Δt = 0.0005 s. The length of the reach is set to be 3.5 km.

Table 1. Computational conditions of 1-D numerical simulation.

Computational Conditions			
Bed slope, θ (degree)	**Potential erosion depth, Dp (m)**	**Rainfall intensity, r (mm/h)**	**Particle diameter, d (m)**
12	2	20	0.10
14	4	40	0.20
16	6	60	
18	10	80	
	15	100	
		120	

In addition to that, the water discharge as the boundary condition are estimated as following.

$$Q = \frac{1}{3.6} frA_{UB} \qquad [27]$$

where Q is the flow discharge, f is rainfall runoff rate (0.82), r is rainfall intensity and A_{UB} is the area of the drainage basin at the upper boundary. To determine the A_{UB}, the area, which has the slope angle of more than 20°, is estimated in the targeted are, with assuming that the saturated non-cohesive sediment cannot be stably exited on the slope. We obtained A_{UB} the in our targeted area as 0.53 km^2, referring to the Chacaito creek.

3.1.2 Results

1-D numerical simulation is conducted to examine the debris flow characteristic, which is the relationship between the debris flow volume and the physical parameters, such as the bed slope, rainfall rates and potential erosion depth, as shown in Table 1.

Firstly, the Figure 2 shows the relation between the debris flow volume and the distance from upper boundary with different slopes when the potential erosion depth is 5 m, particle diameter is 0.2 m, and rainfall intensity is 70 mm/h. As it shows the volume increase progressively as the bed slope increases. As a matter of fact, in the case of 12°, 14°, and 16°, the flow volume increase in between upstream end and few hundred meters, and they have a peak volume around 1,000 m, and keep decreasing thereafter

with very small decreasing rate. On the other hand, the volume increases linearly in the case of 18°. Since the debris flow volume increase by the erosion and deposition, it could say that, in the case of 12°, 14°, and 16°, the erosion processes take place more actively in the upstream reaches, and deposition rate occurred slightly higher than erosion in the downstream reaches. On the other hand, in the case of the slope of 18°, the erosion process is much more active compared with deposition in this whole section.

Figure 3 shows the relationship between the debris flow volume and the distance from upper boundary with different potential erosion depth when particle diameter is 0.2 m, the slope is 15.41°, and rainfall intensity is 60 mm/hour. As it shows, in the case of the potential erosion depth of less than 10 m, the flow volume increase in between upstream end and few hundred meters. After it reaches to the maximum value, the most of the case, it does not change much. On the other hand, in the case with the potential erosion depth of 15 m, it keeps increasing till the downstream end, though increasing rate change at the 100 m from upstream end. They indicates that the erosion already reach to the river bed in the case of the potential erosion depth of less than 10 m. On the other hand, it does not in the case of the potential erosion depth of 15 m. Therefore, the potential erosion depth of 15m is deep enough for sediment transport capacity.

Figure 4 shows the relationship between the debris flow volume and the distance from upper boundary with different rainfall intensity when particle diameter is 0.2 m, the slope is 15.41°, and the potential erosion depth is 5 m. As it shows, the trends of the most of the case are similar with that of Figure 1. They increase rapidly till the distance of around 500 m from upstream end. Thereafter, they decrease very slightly. Overall, the flow volume increase with supply water increases.

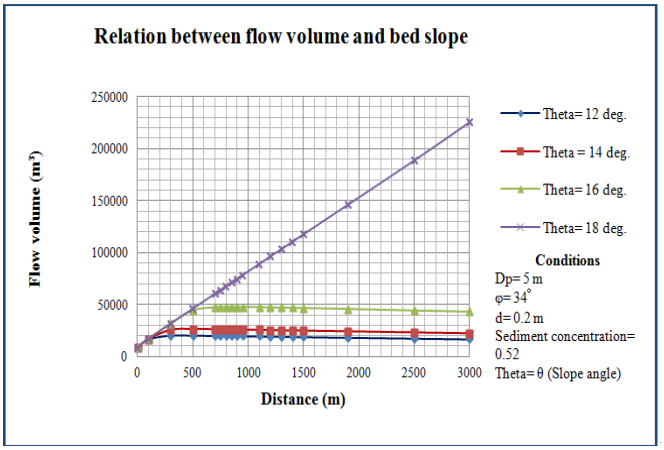

Figure 2: Relation between flow volume and bed slope.

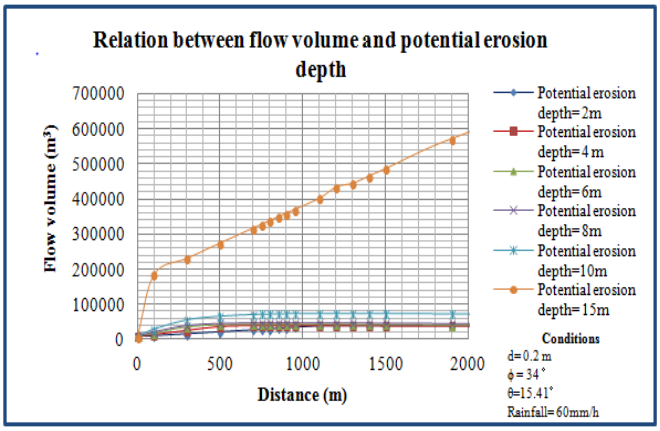

Figure 3: Relation between flow volume and potential erosion depth.

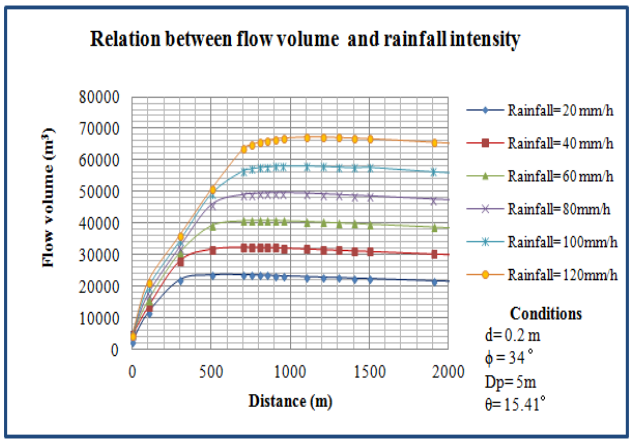

Figure 4: Relation between flow volume and rainfall intensity.

3.2 2-D Numerical simulation

3.2.1 Initial and Boundary condition

To investigate the influences of the bed slope of the debris fan and the supply discharge in spreading process of the debris flow, the 2-D numerical simulation are conducted with assuming the debris fan is laterally flat and inclined only in the flow direction. As the initial condition, three different slope of the debris fan are implemented, such as 4°, 6°, and 8°. As the boundary condition, the supplied debris flow volume including the water and sediment is set to be about 50,000 m^3, whose actual sediment volume is 30,000 m^3. In these computations, steady uniform debris flows in a rectangular open channel are provided from the fan head with three different size with constant volume, in order to discuss about the effects of the velocity. For this purpose, three different expected depth has examined, such as 5.0 m, 7.5 m, and 10.0 m. In addition, the physical parameters are set as same as the 1-D numerical simulation. Δx = 4 m, Δy = 4 m, and Δt = 0.0005 s are applied in this computation.

3.2.2 Results

Figure 5 shows 2-D numerical simulation results as the matrix shape indicating different slope angle in the column and the expectative depth in the row. Each figure indicates the contour map showing the thickness of deposited sediment on the debris fan whose X-Y axis is dimension of the meter. In this figures, the center of outlet of the debris flow are designed as X = 100 m and Y = 200 m. Also each figure indicates the calculation results as deposited area with length and width, as well as the maximum thickness. In the case of slope 4° (Case 11, 21 and 31), the length of sediment distribution decrease approximately 10 m to 16 m, and the width grows from 20 m to 18 m, by each 2.5 m of different expectative depths. Alike, the maximum thicknesses are located in the middle of debris fan. The average of maximum thicknesses value is 5.28 m, where the highest values obtained is in the case 31 (5.54 m) due to the width of sediment distribution is higher and length is smaller than the cases 11 and 21. For the case of 6° and 8°, the length of distribution decrease to rate of 16 m, but the width and the maximum thickness have differences in each case of expectative depth. Notwithstanding these behaviors, the width value increases progressively and the maximum thickness decrease when the depth increases; for example, when the slope is 8°, the debris fan has a great active deposition due to the length values are among 576 m (Case 13) and 534 m (Case 33), with widths are between 80 m and 90 m, and the maximum thickness is 1.17 m.

These results demonstrated that the bed slope influences in the debris flow behavior over the debris fan, because the spatial and temporal distribution of sediment deposition increases due to the highest speeds and the longest distances reach by debris flow when the slope increases but the widths, lengths and heights of deposited sediments where not sensitive to the speeds of the debris flow at the fan head;

however, the simulations were sensitive to slopes of debris fan. Likewise, in the numerical simulation the sediment distribution of deposition is conditioned by the expectative depth.

Slope	Expectative depth (m)		
	5.0 m	7.5 m	10.0 m
4°	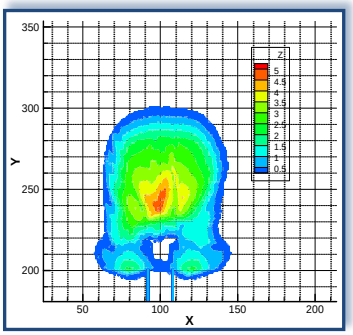	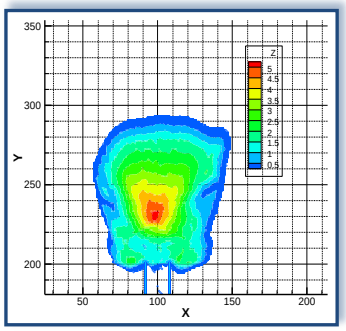	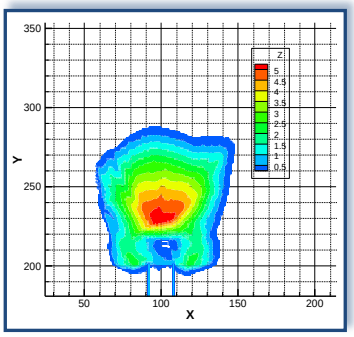
	Case 11	**Case 21**	**Case 31**
	Length, L = 200.00 m Width, W= 150.00 m Maximum thickness, Z=5.13 m	Length, L = 190.00 m Width, W = 170.00 m. Maximum thickness, Z= 5.16 m	Length, L = 174.00 m Width, W= 188.00 m Maximum thickness, Z= 5.54 m
6°	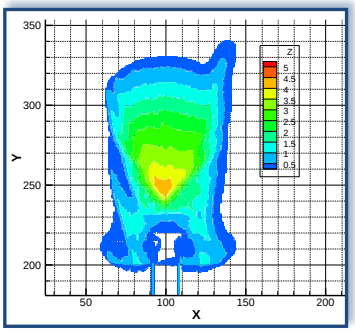	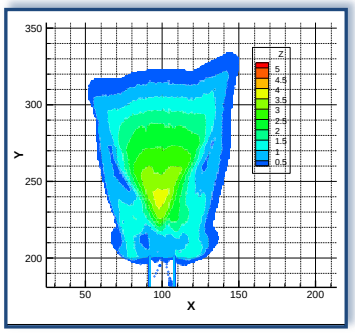	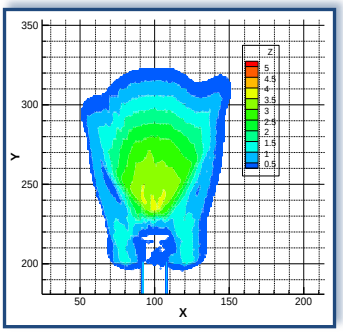
	Case 12	**Case 22**	**Case 32**
	Length, L = 280.00 m Width, W= 168.00 m Maximum thickness, Z= 4.53 m	Length, L = 266.00 m Width, W= 200.00 m Maximum thickness, Z= 3.81 m	Length, L = 244.00 m Width, W= 208.00 m Maximum thickness, Z= 3.77 m
8°	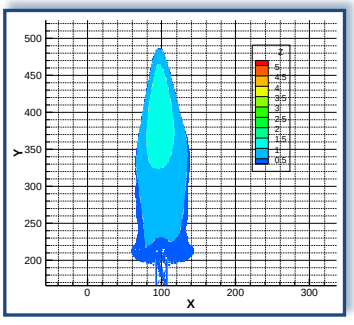	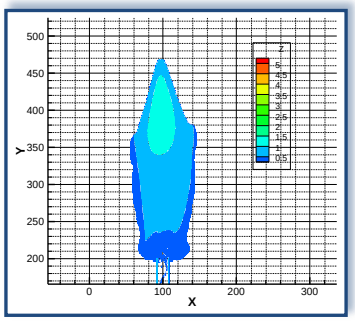	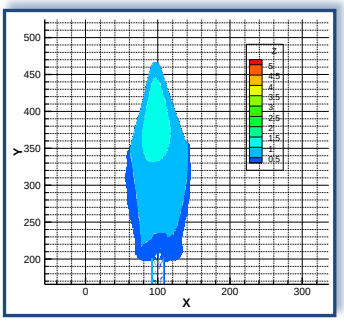
	Case 13	**Case 23**	**Case 33**
	Length, L = 576.00 m Width, W= 80.00 m Maximum thickness, Z= 5.17 m	Length, L = 540.00 m Width, W= 90.00 m Maximum thickness, Z= 1.12 m	Length, L = 534.00 m Width, W= 90.00 m Maximum thickness, Z= 1.13 m

Figure 5: 2-D numerical simulation results. Spatial distribution and thickness of deposition area. Grip size 2 m. Z= [m] Thickness of deposition area.

4. HAZARD MAP

The Chacaito creek is selected for this study to produce the hazard map regarding to the debris flow with 2-D numerical simulation described in the previous chapter. The Chacaito creek basin has an area of 8.43 km^2 and a length profile of 7.79 km. As the Figure 6 indicates, the Chacaito creek has a upper basin located in the mountainous area, which has the average slope of 12°, as well as a lower basin located in the urban area of Caracas city, which has the average slope of 2°. Based on the geometric condition, the debris flow simulation is modeled as the deposited area of debris flow in the lower basin estimated by 2-D numerical simulation, as well as the source area of the debris flow in the upper basin estimated by 1-D numerical simulation.

Figure 6: Chacaito Creek Location. Google Earth, 2013.

The initial condition is established by Digital Elevation Model obtained (DSM) by Civil Protection and Environment Institute of Chacao Municipality, 2012.

The boundary condition regarding to the debris flow in 1-D numerical simulation is designed by means of different returns periods of rainfall intensity, and the estimated discharges are following in the Table 2. Additionally, the physical parameters and other computational conditions used are σ = 2,650 kg/m^3, ρ = 1,000 kg/m^3, d = 0.20 m, ϕ_s = 34°, c_* = 0.52, B = 15 m, Dp = 10 m, Δx = 5.00 m and Δt = 0.005 s.

Table 2. Rainfall intensity according the return period and input discharge estimated for computational conditions of 1-D model. Chacaito creek.

Return period (Years)	25	50	100
Rainfall intensity (mm/h)	48.03	63.81	81.15
Estimated input discharge (m^3/s)	5.36	7.12	9.06

In the case of 2-D numerical simulations, the sediment volume employed is 120,000 m^3 because this value was selected with the flow volumes calculated in 1-D numerical simulations. Also, the computational conditions for 2-D numerical simulation where established same to 1-D numerical simulations. The physical parameters and other conditions employed are following: σ = 2,650 kg/m^3, ρ = 1,300 kg/m^3, d = 0.20 m, ϕ_s = 34°, c_* = 0.30, B = 100 m, Dp = 10 m, Δx = 5.00 m, Δy = 5.00 m and Δt = 0.005 s.

The Figure 7 shows the result of the 2-D numerical simulation, which is the distribution of maximum thickness of debris flow. This figure is drawn to select the maximum deposited height from the results in the different time. The debris flow simulated in the model indicates that, firstly, debris moved to simply downstream as a single stripe, and thereafter, it separated to the west side. Finally it separated to the east side, which is the Chacaito creek. As final form of the deposition of debris flow indicated, the three branches of the deposited sediment appears.

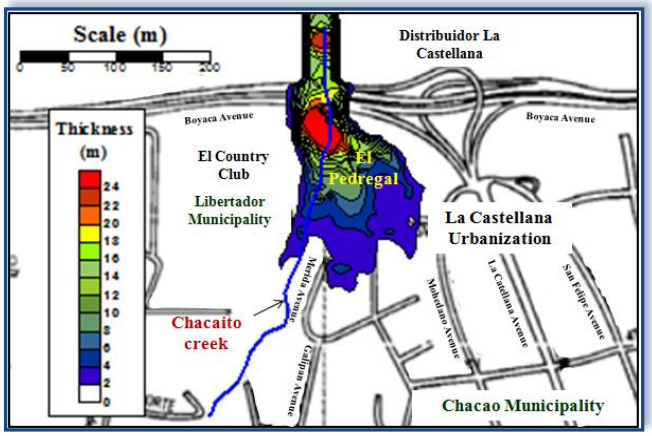

Figure 7: Map of the distribution of maximum thickness of sediment deposition in Chacaito creek

5. CONCLUSIONS

1-D and 2-D numerical simulations were conducted to develop a method for preparing debris flow hazard map. The governing equations used in this research allowed to evaluate debris flow characteristics in the torrents and debris fan. The 1-D simulated results demonstrates that the debris flow volume increases with supply water discharge, length of stream reach and bed slope in condition that potential erosion depth is deep enough for sediment transport capacity of debris flow, and that the debris flow size reaches its equilibrium after flowing over some distance. The 2-D numerical results confirm that the bed slope influences the debris flow behavior over the debris fan and the sediment deposition area, stretches the distance downstream.

In addition, 2-D debris flow behavior was simulated in the debris fan of Chacaito creek and was analyzed, focusing on the thickness of sediment deposition of the flow body. The results shows that the hazardous area spread out over the fan.

6. REFERENCES

Egashira, S. 2007. “Review of research related to sediment disaster mitigation, Journal of Disaster Research, Vol.2, No.1, pp.11-18, 2007.

Egashira, S., 2011. "Experimental study on entrainment of bed material into debris flow". Phys. Chem. Earth (C). Vol. 26 No.9. pp.645-650, 2011.

Egashira, S., Honda, N. and Itoh, T. 2001. "Constitutive equations of debris flow and their applicability". 1st Int. Conf. On Debris-Flow Hazard Mitigation, San Francisco, ASCE, 340-349, 1997.

Egashira, S., Itoh, T., Miyamoto, K. and Honda, N. 1997. "Constitutive equations of debris flow and their applicability". 1st Int. Conf. On Debris-Flow Hazard Mitigation, San Francisco, ASCE, 340-349, 1997

Egashira, S., Itoh, T., Miyamoto, K., 2003. "Debris flow simulation for San Julian torrents in Venezuela". 3rd IAHR Symposium on River, Costal and Estuarine Morphodynamics RCEM, 976-986.

García, R., López, J.L., Noya, M., Bello, M.E., González, N., Paredes, G., Vivas, M.I. & O'Brien, J.S., 2003. Hazard mapping for debris-flow events in the alluvial fans of northern Venezuela. Debris-Flow Hazard Mitigation: Mechanics, Prediction, and Assessment, Rickenmann & Chen (eds). Millpress, Rotterdam, ISBN 90 7717 78 X.

Honda, N. and Egashira, S. 1997. “Prediction of debris flow characteristics in mountain torrents, Proc. 1st Int. Conf. On Debris-Flow Hazard Mitigation, San Fancisco, ASCE, 707-716, 1997.

INE, 2013. "Population census of Bolivarian Republic of Venezuela 2011". Bulletin of National Institute of Statistics. Caracas.

Itoh, T., Miyamoto, K., and Egashira, S., 2003. "Numerical simulation of debris flow over erodible bed". Proceedings of the 3rd International Conference on Debris-Flow Hazards Mitigation, 457-468.

JICA, 2004. Master Plan for Prevention and Attention to Disasters in the Metropolitan District of Caracas.

Mergili, M 2008. Integrated modelling of debris flow with Open Source. Faculty of Geo- and Atmospheric Sciences of University of Innsbruck, Austria.

OBrien, J. S., Julien, P. Y. and Fullerton, W. T. 1993. Two-dimensional water flood and mudflow simulation. Journal of Hydraulic Engineerring 119 (2): 244-261.

Takahashi, T., 2007. Debris flow, mechanics, prediction and countermeasures. Taylor & Francis Group. London.

Takahashi, T., Nakawa, H., Satofuka, Y. and Kawaike., K. 2001. Flood and Sediment Disasters Triggered by 1999 Rainfall in Venezuela; A River Restoration Plan for an Alluvial Fan. Journal of Natural Disaster Science. Vol. 23, Num. 2. pp 65-82.